ORGANOMETALLICS

Article

pubs.acs.org/Organometallics

Alternative Energy Input for Transfer Hydrogenation using Iridium NHC Based Catalysts in Glycerol as Hydrogen Donor and Solvent

Arturo Azua,[†] Jose A. Mata,*[,†] Eduardo Peris,[†] Frederic Lamaty,[‡] Jean Martinez,[‡] and Evelina Colacino*[,‡]

[†]Departamento de Química Inorgánica y Orgánica, Universitat Jaume I, Avda. Sos Baynat s/n, 12071 Castellón, Spain

[‡]Institut des Biomolécules Max Mousseron (IBMM) UMR 5247, CNRS-UM I-UM II Université de Montpellier II, Place E. Bataillon, 34095 Montpellier Cedex 5, France

Supporting Information

ABSTRACT: Four Ir(I) and Ir(III) N-heterocyclic carbene (NHC) based complexes with 3,4,5-trimethoxybenzyl N-substituents have been obtained and fully characterized. The new complexes have been used as catalysts in the reduction of aldehydes and ketones with glycerol, and their activities have been compared to those shown by other Ir(III) NHC-complexes previously reported. The reactions were carried out under oil bath heating, and a detailed comparative study has been carried out using microwave (MW) and ultrasound (US) activation. The new Ir(III) complexes proved to be most efficient in the reduction of ketones, while the Ir(I) complexes are more active in the reduction of aldehydes. The use of ultrasound has a tremendous impact in shortening reaction times, and good results have been obtained in the reduction of aldehydes. In some experiments transmision electron microscopy (TEM) and UV−vis analysis showed the presence of iridium-containing nanoparticles after MW or US activation.

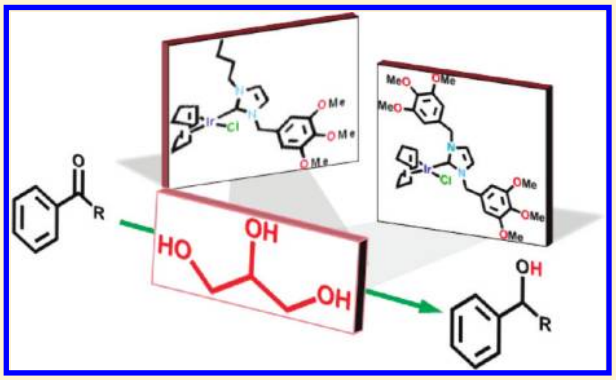

INTRODUCTION

The current search for energy-saving and more selective protocols has turned ultrasound and microwave into useful alternatives to prolonged heating in metal-catalyzed reactions.[1] In particular, these two nonconventional activation tools have been widely used in many palladium-catalyzed reactions,[1b,c,2] for which substantial benefits may be found, including reduced reaction times and improved yields and selectivity. The science of green chemistry was developed to meet the increasing demand for environmentally benign chemical processes. In this regard, the combination of efficient catalytic protocols and environmentally friendly solvents are of importance in the search for laboratory-scale syntheses. Although many solvents meet the green chemistry criteria, glycerol has recently caught the attention of many researchers, due to its unique physical and chemical properties and its extraordinarily low cost and ready availability.[3] Apart from its use as a solvent, new and innovative catalytic processes based on the use of glycerol have recently been developed,[4] including its use as an environmentally friendly hydrogen donor for transfer hydrogenation (TH) reactions.[5]

Transfer hydrogenation (TH) is a metal-catalyzed process during which hydrogen is transferred from an alcohol (2-propanol or cyclopentanol) to an unsaturated bond. With respect to the conventional hydrogenation reaction using the highly flammable molecular hydrogen, TH is a safer and more valuable atom-efficient, environmentally benign method, in which the alcohol acts as both the reaction solvent and the source of hydrogen.

In a number of recent examples, glycerol has replaced 2-propanol as a hydrogen source in ruthenium-catalyzed TH reactions.[5b−d,6] The experiments were carried out in an oil bath (OB) or using a domestic microwave (MW) oven. Generally, the efficiency of all processes was low, and high catalyst loadings and long reaction times (6−24 h) were required for achieving acceptable substrate conversion. Better results were obtained when oil bath (OB) or microwave (MW) heating were used in combination with ultrasound (US) activation.[6b] However, TH reactions in glycerol catalyzed by iridium-based catalysts have been scarcely investigated.[5a,e,7] The efficiency of these organoiridium derivatives functionalized with NHCs,[5e] N−N ligands,[5a] or P−N[7] was evaluated by heating the reaction mixture in an oil bath, and in some cases the use of a cosolvent was required.[7]

In our search for efficient catalysts for hydrogen-borrowing processes,[8] we recently reported the use of a series of Ir NHC based catalysts (**1**−**3**, Figure 1) for the reduction of organic carbonyl compounds, using glycerol as both solvent and hydrogen donor.[5e] On the basis of previous findings, we now report the preparation of new Ir(I) and Ir(III) NHC based catalysts (**4** and **5**, Figure 1), which have been used in the transfer hydrogenation of different carbonyl compounds, using

Received: February 10, 2012
Published: May 7, 2012

   dx.doi.org/10.1021/om300109e | *Organometallics* 2012, 31, 3911−3919

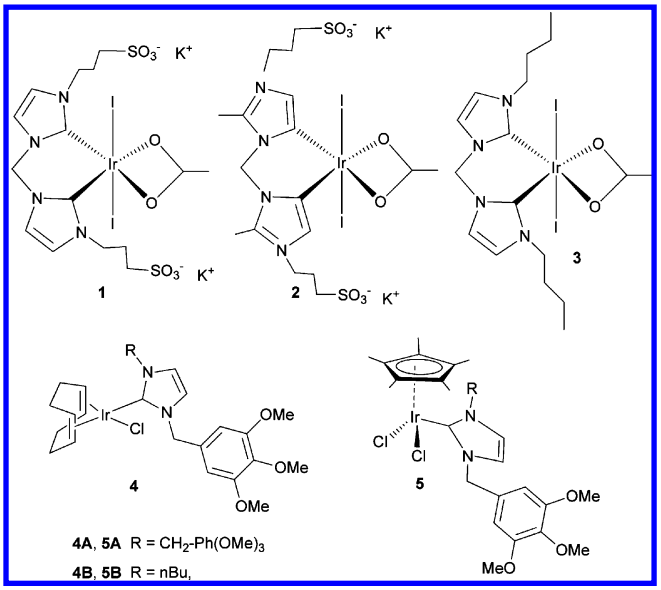

Figure 1. Ir(III) and Ir(I) NHC based catalysts for transfer hydrogenation reactions.

glycerol as reducing agent and solvent (Scheme 1). The catalytic properties of these new complexes have been

Scheme 1. Iridium-Catalyzed Transfer Hydrogenation Reactions of Carbonyl Compounds

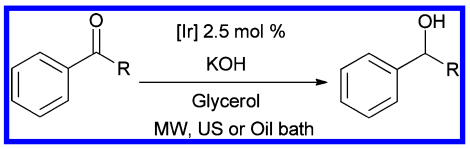

compared with those previously obtained.[9] In order to establish the greenest and most efficient catalytic protocol, we have performed the reactions under microwave and ultrasound conditions, and the results were compared with those obtained by the conventional oil-bath heating procedure.

RESULTS AND DISCUSSION

Iridium(III) complexes of general formula $[IrOAcI_2(bis\text{-}NHC)]$ (**1**–**3**, Figure 1) were prepared as previously described.[9] Imidazolium ligand precursors were readily accessible by alkylation of commercial available N-alkylimidazoles or by following previously described procedures.[10] Imidazolium salt **A** (Scheme 2) is a symmetrical salt with two trimethoxybenzyl groups,[11] while imidazolium salt **B** is asymmetrical with one trimethoxybenzyl group and an *n*-butyl group. The products are colorless and hygroscopic with spectral properties similar to those of other reported imidazolium salts. The iridium NHC based complexes were obtained by transmetalation from the corresponding silver carbene derivatives by a two-step process (Scheme 2). The first step involves the deprotonation of the imidazolium salt with silver oxide to form the silver-NHC complex. We used this complex in situ without isolation. In the second step, after the addition of $[IrCl(COD)]_2$ immediately a white precipitate of silver chloride was formed, indicating the formation of the iridium NHC complexes in good yields (80% **4A** and 78% **4B**). Following the same procedure but using $[IrCp^*Cl_2]_2$ as metal

Scheme 2. Synthesis of Iridium NHC Based Catalysts

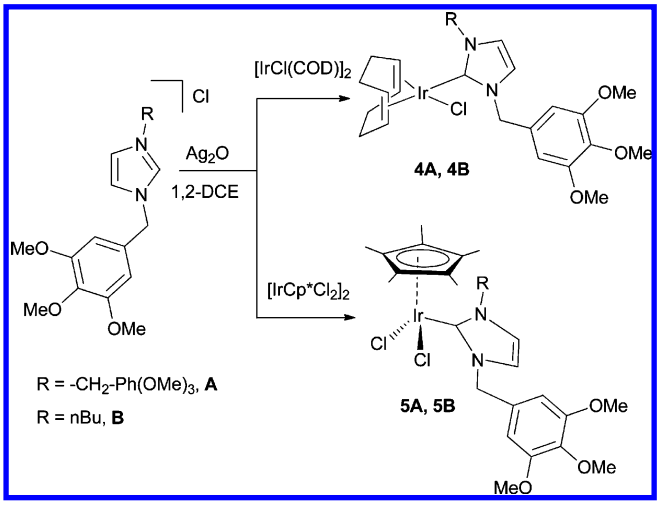

precursor, complexes **5A,B** were obtained (75% **5A** and 55% **5B**) (Scheme 2).

Positive ion ESI-MS analysis of the isolated products **4** and **5** in MeCN showed an intense peak for $[M - Cl]^+$ (m/z 729 for **4A**, m/z 605 for **4B**, m/z 791 for **5A**, and m/z 667 for **5B**). The second highest peak in intensity for complexes **4** corresponds to the fragment which coordinates a molecule of acetonitrile $[M - Cl + MeCN]^+$ (m/z 770 for **4A** and m/z 646 for **4B**). This fragment was not observed in the Ir^{III} complexes **5**. HRMS analysis of complexes **4** and **5** showed a good agreement between the simulated and theoretical spectra, with relative errors of less than 2 ppm, confirming the proposed nature of these complexes (see the Supporting Information for details).

X-ray Diffraction Studies. Crystals of **4A,B** and **5A** suitable for X-ray diffraction were obtained by slow evaporation from corresponding concentrated dichloromethane–hexanes solutions. Figures 2–4 show the molecular diagrams of the iridium complexes with the atom-numbering scheme and the selected bond lengths (Å) and angles (deg). The geometry at iridium of **4A** (Figure 2) is square planar. This iridium coordination plane is almost perpendicular to the plane angle defined by the azole ring (α = 85.8°). The Ir–C(carbene) bond length is 2.015(8) Å, as expected for NHCs. The trimethoxybenzyl groups point away from the metal center, just avoiding steric repulsion with the cyclooctadiene (COD) and chlorine ligands. The molecular structure of **4B** is similar to that of **4A** (Figure 3). The Ir–C(carbene) bond length is 2.031(3) Å, and the α angle is 86.0°.

The molecular structure of compound **5A** (Figure 4) has a symmetrically substituted NHC ligand coordinated to the metal center. Two chlorides and a Cp* ligand complete the coordination sphere about the Ir(III) center. The Ir–C(carbene) distance is 2.061 Å. The two bulky 3,4,5-trimethoxybenzyl N substituents point out of the coordination sphere, minimizing the steric interaction.

Catalytic Studies. In our search of new methodologies using glycerol activation, we have observed previously that complexes **1**–**3** are very efficient in transfer hydrogenation processes under oil bath heating.[5e] The Ir(III) complexes **1** and **2**, with a chelating bis-NHC ligand and sulfonate groups, were the most active, probably due to their high solubility in the reaction media (see Figure 1 in the Supporting Information) and to the strong electron-donor properties of the bis-carbene

dx.doi.org/10.1021/om300109e | *Organometallics* 2012, 31, 3911–3919

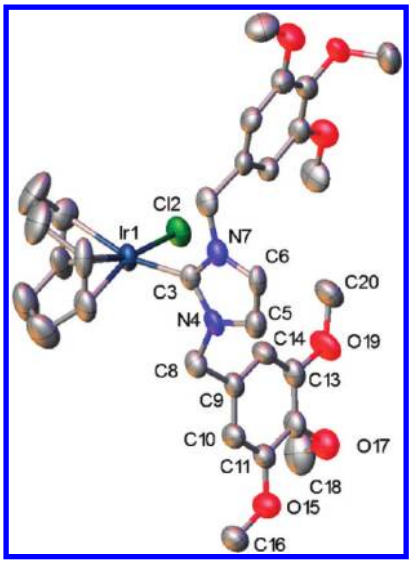

Figure 2. Molecular diagram of complex **4A**. Ellipsoids are given at the 50% probability level. Hydrogens are omitted for clarity. Selected bond lengths (Å) and angles (deg): Ir(1)−C(3) = 2.015(8), Ir(1)−Cl(2) = 2.372(2), Ir(1)−C(35) = 2.094(9), C(3)−N(4) = 1.366(11), N(4)−C(8) = 1.462(11); C(3)−Ir(1)−Cl(2) = 89.4(2), C(3)−N(4)−C(8) = 124.1(8), C(11)−O(15)−C(16) = 117.1(7). α = 85.8° (α = angle between the iridium coordination plane and the azole ring plane).

ligands, especially for catalyst **2** with the abnormally bound bis-NHC ligand.

As a starting point of our investigation, we explored the catalytic performances of the novel prepared Ir(I) (**4B**) and

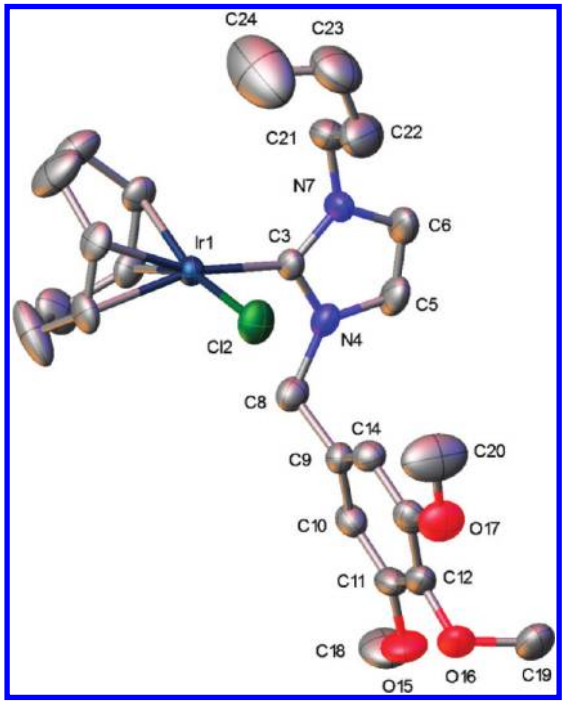

Figure 3. Molecular diagram of complex **4B**. Ellipsoids are given at the 50% probability level. Hydrogens are omitted for clarity. Selected bond lengths (Å) and angles (deg): Ir(1)−C(3) = 2.031(3), Ir(1)−Cl(2) = 2.3581(9), Ir(1)−C(25) = 2.166(3), C(3)−N(4) = 1.357(4), N(4)−C(8) = 1.460(5); C(3)−Ir(1)−Cl(2) = 88.22(9), C(3)−N(4)−C(8) = 124.2(3), C(12)−O(16)−C(19) = 114.0(3). α = 86.0° (α = angle between the iridium coordination plane and the azole ring plane).

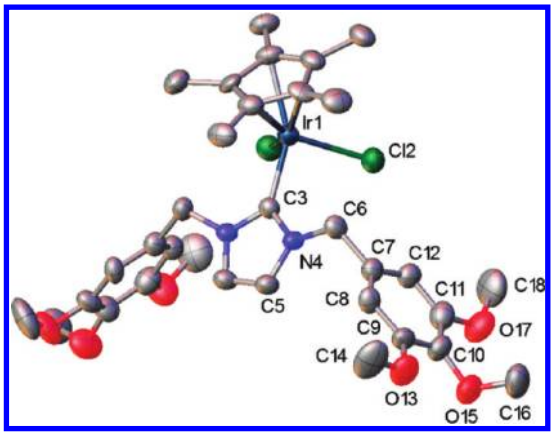

Figure 4. Molecular diagram of complex **5A**. Ellipsoids are given at the 50% probability level. Hydrogens are omitted for clarity. Selected bond lengths (Å) and angles (deg): Ir(1)−C(3) = 2.061(11), Ir(1)−Cl(2) = 2.428(2), Ir(1)−Cp(cent) = 1.979, C(3)−N(4) = 1.356(9), N(4)−C(5) = 1.384(10); C(3)−Ir(1)−Cl(2) = 90.8(2), C(3)−N(4)−C(5) = 111.5(7), C(3)−N(4)−C(6) = 124.5(7).

Ir(III) (**5A**, **5B**) catalysts, bearing nonionic polar groups, in TH reactions in an oil-bath, using benzaldehyde and acetophenone as substrates. Their efficiency was compared with that of catalysts **1**−**3**, having ionic polar sulfonate functionalities. Table 1 summarizes the data that we obtained.

Table 1. Selected Data for Transfer Hydrogenation in Oil Bath (OB)[a]

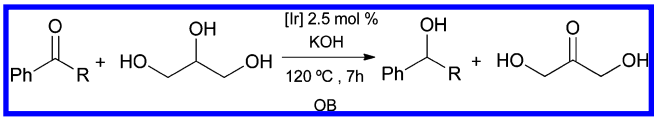

entry	cat.	R	yield (%)[b]
1	**1**	H	66
2	**2**	H	99
3	**4B**	H	71
4	**5A**	H	98
5	**5B**	H	91
6	**1**	Me	45
7	**2**	Me	69
8	**3**	Me	25
9	**4B**	Me	80
10	**5A**	Me	40
11	**5B**	Me	35

[a]Reactions were carried out with 0.5 mmol of substrate, KOH (0.5 mmol), and 0.8 mL of glycerol at 120 °C for 7 h. Anisole (0.5 mmol) was used as internal standard. [b]Yields determined by GC on the basis of 1-phenylethanol or benzyl alcohol production.

In a typical experiment acetophenone (or benzaldehyde), potassium hydroxide, the catalyst (2.5 mol %), and glycerol were heated at 120 °C for 7 h (Table 1). Acetophenone is reduced to 1-phenylethanol and benzaldehyde to benzyl alcohol, while glycerol is dehydrogenated to dihydroxyacetone (DHA), a compound which is extensively used in the cosmetics industry as a sunless tanning compound. Under the reaction conditions used, DHA partially decomposes, as previously demonstrated.[5b,7]

As seen from the data shown in Table 1, all the Ir(I) and Ir(III) catalysts were active in the reduction of carbonyl groups with moderate to excellent yields, depending on the catalyst

dx.doi.org/10.1021/om300109e | *Organometallics* 2012, 31, 3911−3919

used, but with the advantage that no additive or cosolvent was required, differently than similar iridium-catalyzed transformations.[5a] Catalysts **2** and **5A** afforded excellent catalytic performances in the reduction of benzaldehyde (Table 1, entries 2 and 4), while catalysts **2** and **4B** afforded the best catalytic performances in the reduction of acetophenone (Table 1, entries 7 and 9). The very low activity displayed by catalyst **3** in the reduction of acetophenone (Table 1, entry 8) may be due to its poor solubility, in comparison to that shown by the sulfonate-substituted complex **1** (Table 1, entry 6).

A yield vs time plot for benzaldehyde reduction in glycerol was evaluated using catalysts **4B** and **5A**, **5B** (Figure 5). The

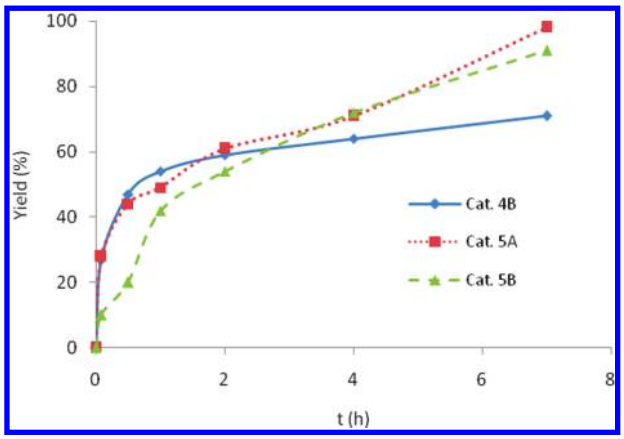

Figure 5. Time course of benzaldehyde reduction in glycerol. Conditions: 2.5 mol % catalyst, 0.5 mmol of benzaldehyde, KOH (0.5 mmol), 0.8 mL of glycerol at 120 °C. Anisole (0.5 mmol) was used as internal standard. Yields were determined by GC.

reaction was very clean, and we did not observe any other side products apart from benzyl alcohol. All catalysts employed were very active at short times, reaching 50% yield after 1 h. The best catalyst is **5A**, reaching almost quantitative yields (98%) within 7 h. The absence of an induction period before initiation of the catalytic process is in agreement with the higher initial activity expected for catalysts with electron donor NHC ligands.

However, rationalization of these data is not obvious, taking into account only the catalyst solubility in glycerol. Electron-releasing ligands were expected to produce more active catalysts, while COD complexes were poorly soluble in glycerol, and several other factors affect the TH reaction: (i) the ligand steric hindrance on the coordination of the reactants and the products, (ii) the kinetics of catalyst deactivation, (iii) poor mass and heat transport in glycerol, and (iv) the solubility of all reactants.

The iridium-catalyzed transfer hydrogenation most probably goes through the "hydridic route", involving a monohydride.[9a,12] In the first step, an iridium alkoxide is formed after the deprotonation of glycerol in basic medium (Scheme 3). This intermediate evolved to the formation of an iridium hydride intermediate with a β-hydrogen elimination of dihydroxyacetone (DHA), followed by the insertion of the carbonyl substrate into the iridium–hydride bond to give an alkoxide. In the final step, the product is obtained after an alkoxide exchange step in which a second molecule of glycerol enters the metal coordination sphere, regenerating the catalytic species. The base plays a double role: to activate the metal complex by abstracting the acidic proton of the hydrogen donor[13] and to assist in proton dissociation from the hydroxyl group of the

Scheme 3. Plausible Mechanism for Iridium-Catalyzed Transfer Hydrogenation Reactions in Glycerol

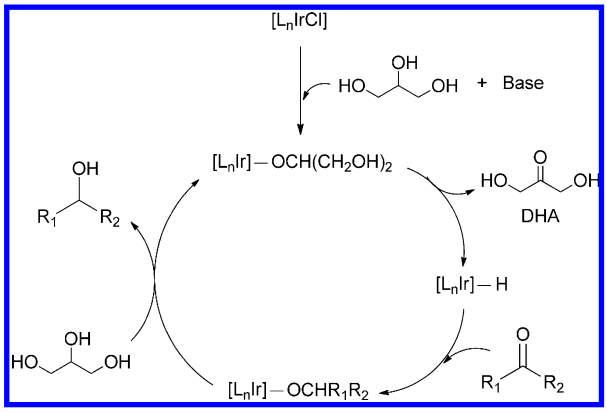

alcohol. Introduction of electron donor NHC ligands may produce the enhancement of the catalytic activity through the increase of the nucleophilicity of the iridium hydride intermediate, leading to a more facile interaction with the electrophilic carbonyl substrate.

The use of glycerol as the reaction solvent presents some drawbacks such as the low solubility of highly hydrophobic molecules and gases, such as hydrogen and oxygen. Its high viscosity does not facilitate the diffusion of substrates and catalyst. These limitations may be overcome by performing the reactions under microwave (MW)[1i,14] or high-intensity ultrasound (US)[6b,15] activation.

Because of its intrinsic characteristics such as high boiling point (T = 290 °C), low vapor pressure (0.0025 mm at 50 °C), high dielectric constant (ε = 42.48 at 25 °C), and a polarity similar to that of other organic solvents such as DMSO and DMF, glycerol can be used as a suitable solvent for microwave irradiation,[1i] where the heating characteristics of the solvent play a crucial role. Moreover, the recovery of the final products is simplified by simple decantation of the crude reaction mixture with glycerol-immiscible solvents (e.g., Et_2O or cyclohexane).

In an unprecedented study, the iridium-catalyzed TH reaction was investigated under microwave irradiation in a chemistry-dedicated microwave apparatus, in closed vessels. Selected data and conditions are summarized in Table 2. Reduction of the carbonyl group (benzaldehyde or acetophenone) into the corresponding alcohols could be achieved in short reaction times (1–2 h) and relatively low temperatures (80–120 °C) in good yields (60–95%) under microwave activation. Catalyst **2** displayed the best activity in the reduction of benzaldehyde (Table 2, entries 1–5) in glycerol as well as in a comparative experiment using 1,2-propanediol as hydrogen donor (Table 2, entry 2). Very low conversion of substrate (30%) and poor yield of benzyl alcohols (35%) were observed on heating the mixture in poly(ethylene glycol) (average molecular weight ca. 300 Da). At 120 °C, no improvement was possible by the presence of a cosolvent (DMSO) or by doubling either the reaction times or the catalyst loading (5 mol %). The use of AgOTf as additive was detrimental, leading to the formation of many byproducts.

The heating mode of the sample and the magnetron power set to reach the selected instruction (T = 120 °C) seemed to be important parameters (see Figure 3 in the Supporting Information). When the initial starting heating power was off (Table 2, entry 3), the yield was moderate. The results were

dx.doi.org/10.1021/om300109e | *Organometallics* 2012, 31, 3911–3919

Table 2. Selected Data for Transfer Hydrogenation Processes under Microwave Irradiation (MW)[a]

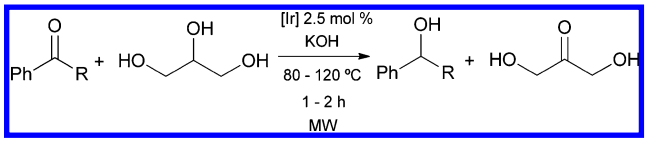

entry	cat.	R	T (°C)	t (h)	yield (%)[a,b]
1	**2**	H	80	2	60
2[c]	**2**	H	80	2	70
3[d]	**2**	H	120	1	32
4[e]	**2**	H	120	1	68
5[f]	**2**	H	120	1	95
6	**4B**	H	120	1	13 (54)[g]
7	**5A**	H	120	1	20 (49)[g]
8	**5B**	H	120	2	22 (54)[g]
9[f]	**2**	Me	120	1	83
10	**2**[h]	Me	200	2	77
11		Me	120	2	0

[a]Reactions were carried out with 0.5 mmol of substrate, KOH (0.5 mmol), and 0.8 mL of glycerol. Anisole (0.5 mmol) was used as internal standard. [b]Yields were determined by GC on the basis of 1-phenylethanol or benzyl alcohol produced. [c]Using 0.8 mL of 1,2-propanediol instead of glycerol. [d]Starting heating power off. [e]Simultaneous cooling system, with starting heating power off. [f]Starting heating power set at its maximum level (400 W). [g]Yields in parentheses are given for experiments carried out in an oil bath at 120 °C. [h]1 mol % of catalyst **2**.

improved by heating the mixture with the technique of simultaneous cooling (Table 2, entry 4), introducing higher levels of MW energy into the reaction vessel[16] even if the initial starting heating power was set to off (see Figure 4 in the Supporting Information). When the starting heating power was set at its maximum level (400 W) (Table 2, entry 5), high yields of reduced products were obtained.

Disappointingly, catalysts **4B**, **5A**, and **5B** were ineffective under microwave heating, giving better results under oil bath heating, most probably due to some degree of catalyst decomposition under microwaves (Table 2, entries 6–8). When acetophenone was the substrate, catalyst **2** was the most efficient (Table 2, entries 9 and 10). Despite the fact that comparable yields of 1-phenylethanol were obtained, it is not possible to determine if the reaction was driven by thermal or nonthermal microwave effects.[17]

MW results can be analyzed on the basis of different factors, related not only to the relative solubility of substrate and catalyst in glycerol phase, the viscosity of the medium, and the diffusion properties of the compounds but also the microwave absorption of the medium. This is also a function of the hydration layer thickness surrounding the glycerol and/or molecules,[18] glycerol being able to absorb moisture from the atmosphere, with unpredictable consequences on organometallic catalysis.

Since this reaction with NHC-based iridium catalysts was unexplored under ultrasound activation,[6b] complexes **1**–**5** were then evaluated in transfer hydrogenation with the same model substrates using ultrasound activation. Parameters such as reaction time, catalyst loading, temperature, and wave amplitude were screened for each catalyst, and the selection of the best data is reported in Table 3. Catalyst **4A** displayed the best results in the reduction of benzaldehyde: the reaction is fast and selective at the beginning, and the yield is good in a

Table 3. Selected Data for Transfer Hydrogenation Processes under Ultrasound Irradiation (US)[a]

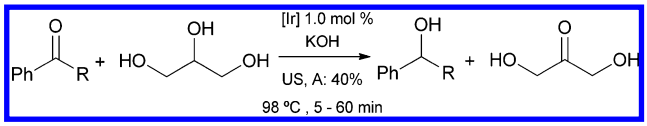

entry	cat.	R	T (°C)	t (min)	yield (%)[b]
1	**1**	H	98	5	49
2	**2**	H	60	60	35
3	**2**	H	98	5	55
4[c]	**2**	H	98	5	25
5[d]	**2**	H	98	5	20
6[e]	**2**	H	98	5	30
7[f]	**2**	H	80	20	64
8	**4A**	H	98	5 (30)[g]	73 (11)[g]
9	**4B**	H	98	5 (900)[g]	40 (7)[g]
10	**5B**	H	98	10 (10)[g]	45(25)[g]
11	**1**	Me	80	25(900)[g]	34(40)[g]
12[f]	**2**	Me	80	60(900)[g]	60(68)[g]
13	**2**	Me	40	30	56
14[h]	**2**	Me	40	40	21
15	**4A**	Me	80	30	20
16	**4B**	Me	80	20	20
17	**5A**	Me	80	30	22

[a]Reactions were carried out with 0.5 mmol of substrate, KOH (0.5 mmol), 0.8 mL of glycerol, and an amplitude of 40%. Anisole (0.5 mmol) was used as internal standard. [b]Yields determined by GC based on 1-phenylethanol or benzyl alcohol produced. [c]Using 0.4 mL of glycerol and 0.4 mL of DMSO. [d]Using 0.4 mL of glycerol and 0.4 mL of H_2O. [e]Using 0.4 mL of glycerol and 0.4 mL of PEG_{300}. [f]2.5 mol % cat. [g]Data in parentheses are given for experiments carried out in an oil bath at 90 °C. [h]The amplitude was 20%.

very short time (5 min) and with low catalyst loading (Table 3, entry 8). This is maybe due to an optimal dispersion of the base in glycerol, as well as excellent cavitation, producing a microenvironment (microbubbles) where the reaction takes place.

As a general trend, when the catalyst loading was increased (2.5 mol %, Table 3 entry 7) or the reaction time extended to up to 1 h (Table 3, entry 2), no pronounced decrease of the substrate could be observed but other byproducts were observed in the crude mixture together with benzyl alcohol, perhaps due to the formation of cyclic acetals between glycerol and benzaldehyde.

The addition of a cosolvent such as DMSO, H_2O, and PEG_{300} did not improve the catalytic outcomes (Table 3, entries 4–6). Because the transfer hydrogenation is an equilibrium reaction, we also tried to use a larger excess of hydrogen donor (glycerol), to displace the equilibrium toward the product side, but the results were not improved.

The bis-NHC abnormally bound **2** was the most efficient for the reduction of acetophenone (Table 3, entry 12). However, the amplitude of the ultrasound wave seems to have an effect on the yield (Table 3, entries 13 and 14). The ultrasound beam experienced a loss of energy when traveling through the medium. The input signal amplitude can be adjusted to compensate this loss of energy, modifying the energy content, or "strength" of the ultrasound pulse. The optimum could be obtained with an amplitude of 40%, allowing a much greater energy to be delivered. The low yields obtained in the other cases could be rationalized in terms of a partial deactivation of the catalyst, probably due to an ultrasound-induced mod-

dx.doi.org/10.1021/om300109e | *Organometallics* 2012, 31, 3911–3919

ification of the structure of the catalytic site or by the presence of the coordinating chloride counteranion slowing the formation of the active [Ir]-H intermediate under these conditions. It is worth noting that comparative experiments using an oil bath at the same temperature (Table 3, entries 8−12) proved to be ineffective even after prolonged heating. This is not so surprising, as the effect of sonication is explained in terms of "hot spots" theory, and hundreds of atmospheres are generated by the collapse of cavitation bubbles responsible for the chemical reactions.[19] No similar bubble formation is possible under conventional oil bath heating or during microwave irradiation.

During the reaction the solution turned into a homogeneous dark brown suspension. Glycerol is a strong reducing agent of the metallic center, leading to nanoparticles (polyol method).[20,21] The glycerol phase recovered after microwave or ultrasound irradiation was analyzed by transmission electron microscopy (TEM), showing the formation of iridium-containing nanoparticles (Figure 6). It is important to point out that the formation of these nanoparticles resulted in the deactivation of the catalytic process; this is not unexpected,[22] especially under ultrasound activation where strong cavitation phenomena occur in a viscous medium such as glycerol.

The TEM analysis of the glycerol phase obtained in the experiment carried out under microwave irradiation with the starting heating power set at its maximum level (400 W) (Table 2, entry 5) showed the formation of a dispersion of spherical iridium-containing nanoparticles with uniform and narrow size distribution (ca. 2−3 nm), free of sintering, throughout the grid (Figure 6a). The TEM analysis of glycerol phase obtained after microwave irradiation with the technique of simultaneous cooling, while keeping the starting heating power off (Table 2, entry 4), showed again the formation of similar shaped iridium-containing nanoparticles (ca. 2−3 nm), homogeneously distributed (sintering-free) but in a lower concentration (Figure 6b). This observation may be explained by the different heating profile, under microwave irradiation, since at the early beginning of the reaction (see Figure 3 in the Supporting Information), before that the set value (T = 120 °C) is reached. This may influence the kinetics of nucleation, that would be probably retarded in the case of a simultaneous cooling method. To our knowledge, iridium nanoparticles have never been previously synthesized using glycerol under microwave activation. We have observed that glycerol/ultrasound synergy allowed an effective and fast nucleation of iridium-containing nanoparticles in only 5 min (Figure 6c and Table 3, entry 8). The particles are homogeneously spread throughout the support with a narrow size distribution of ca. 3−5 nm.

Iridium-containing nanoparticles were examined with ultraviolet−visible (UV−vis) spectroscopy (Figure 7). The iridium nanospheres showed a small intense band at 270 nm similarly to previous reports[23] for metallic iridium formed under reducing conditions, which in our case is provided by the use of glycerol. It is out the scope of the present study to investigate the physical mechanism leading to nanoparticle formation and growth.

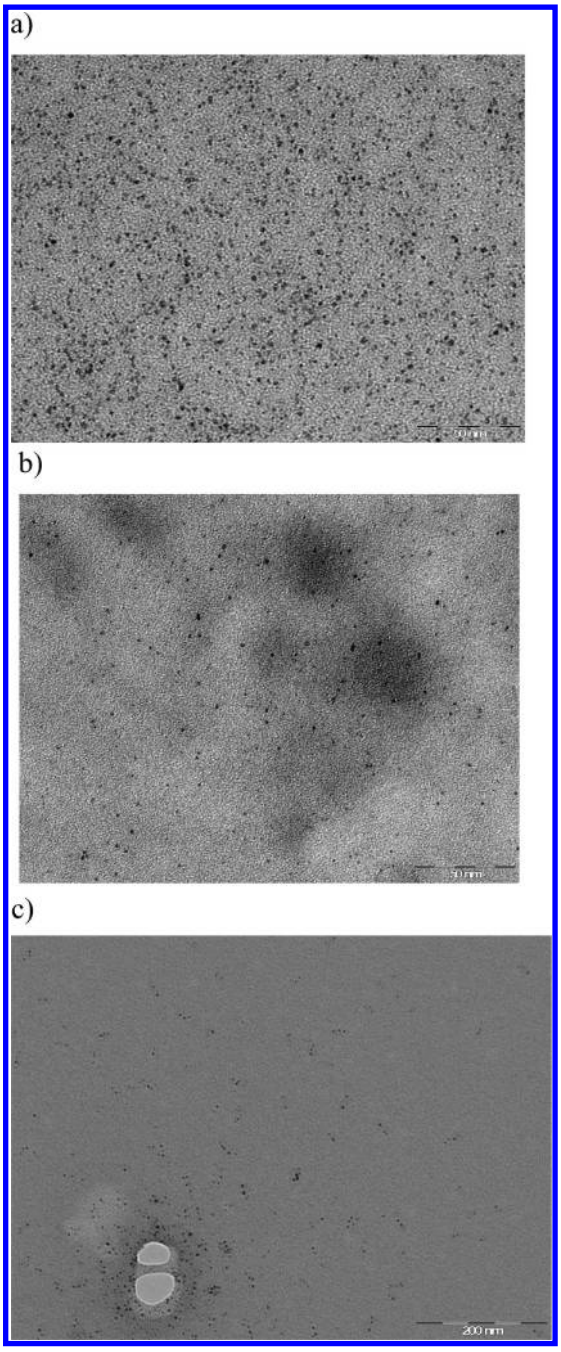

Figure 6. TEM micrographs for iridium-containing nanoparticles synthesized (a) under MW irradiation using catalyst **2** with starting heating power set at its maximum level (400 W), (Table 2, entry 5), (b) under MW irradiation using catalyst **2** with simultaneous cooling system and starting heating power off (Table 2, entry 4), and (c) under US irradiation using catalyst **4A** (Table 3, entry 15).

■ CONCLUSIONS

Novel iridium NHC based complexes have been synthesized and fully characterized. The easy modulation of the NHC ligands leads to physical differences in the catalyst properties such as solubility. The catalytic properties have been evaluated and compared with those of previously reported iridium complexes in the transfer hydrogenation reaction using glycerol as solvent and hydrogen donor under microwave, ultrasound and oil bath conditions. In particular, the ultrasound gains a special place as a promising heating technique for developing new catalytic processes in glycerol. The formation of spherically shaped Ir(0)-containing nanoparticles in glycerol was demonstrated, using microwave or ultrasound heating. Glycerol is a cheap, nontoxic, biodegradable, and easily available byproduct in biodiesel fuel production, obtained from the saponification of triglycerides of all natural fats and oils. Due to the its industrial

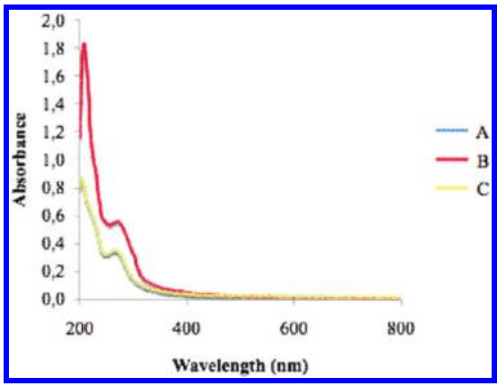

Figure 7. UV−vis absorption spectra of iridium-containing nanoparticles: (A) catalyst **2** under MW irradiation with starting heating power set at its maximum level (400 W); (B) catalyst **2** under MW irradiation with simultaneous cooling system and starting heating power off; (C) catalyst **4A** under US irradiation.

importance as the intermediate of many valued fine chemicals, as well as the solvent of choice for many industrial and pharmaceutical preparations (foods, cosmetics, liquid detergents, antifreeze), new methodologies are being developed in our laboratories for a green and sustainable chemistry in glycerol.

EXPERIMENTAL SECTION

General Procedures. Compounds **1**−**3** and imidazolium salt A were prepared according to literature procedures.[9a−c,11] All experiments were carried out under nitrogen using standard Schlenk techniques and high vacuum, unless otherwise stated. Anhydrous solvents were dried using a solvent purification system (SPS MBraun). All other reagents were used as received from commercial suppliers. Glycerol was used as received from Sigma-Aldrich (ref. no. G9012, >99%). The products were identified by a GCMS-QP2010 (Shimadzu) gas chromatograph/mass spectrometer equipped with a Teknokroma (TRB-5MS, 30 m × 0.25 mm × 0.25 mm) column, and the spectra obtained were compared with the standard spectra. Yields, conversion, and product selectivity were determined by a GC-2010 (Shimadzu) gas chromatograph equipped with an FID and a Teknokroma (TRB-5MS, 30 m0.25 mm 0.25 mm) column. NMR spectra were recorded on Varian spectrometers operating at 300 or 500 MHz (^{1}H NMR) and 75 and 125 MHz (^{13}C NMR), respectively, and referenced to $SiMe_4$ (δ in ppm and J in hertz). NMR spectra were recorded at room temperature with the appropriate deuterated solvent ($CDCl_3$, CD_3OD, or d_6-DMSO). The identity of analytically pure samples of the saturated alcohols was assessed by comparison of their ^{1}H NMR data previously described in the literature and by their fragmentation in GC/MS. Microwave-assisted reactions were performed in sealed vessels with a Biotage Initiator 60 EXP instrument. The temperature was measured with an IR sensor on the outer surface of the reaction vial. Open vessel sonochemical reactions were performed in probe systems (VCX-400 Sonics Materials Vibracell) equipped with an immersion horn made from titanium alloy. The working frequency was 20 kHz, using 40% amplitude. Analytical high-performance liquid chromatography (HPLC) was performed on a Waters Millenium 717 equipped with an Autosampler, with a variable-wavelength diode detector using a Chromolith RP18 column (50 × 4.6 mm), flow 5 mL/min, linear gradient CH_3CN in water 0−100% (+ 0.1% TFA) in 4.5 min. Transmission electron microscopy (TEM) micrographs were recorded on a JEOL 1200EX2 (Tokyo, Japan, 1990) at an operating voltage of 100 kV. Particles were dispersed in ethanol (microwave experiments) or in water (ultrasound experiments) by ultrasonication for 30 min, loaded on carbon-coated copper grids (300 mesh), and allowed to dry at room temperature before recording the micrographs. UV−vis spectra were recorded using a Jenvay 7315 scanning spectrophotometer with quartz cells of 1 cm path length.

X-ray studies. Diffraction data were collected on a Agilent SuperNova diffractometer equipped with an Atlas CCD detector using Mo Kα radiation (λ = 0.710 73 Å). Single crystals were mounted on a MicroMount polymer tip (MiteGen) in a random orientation. Absorption corrections based on the multiscan method were applied.[24] Structures were solved by direct methods in SHELXS-97 and refined by the full-matrix method based on F^2 with the program SHELXL-97 using the OLEX software package.[25]

Catalytic Studies. *General Method for TH in an Oil Bath.* In a typical experiment of transfer hydrogenation using glycerol as hydrogen donor, a capped vessel containing a stirrer bar was charged with the substrate (0.5 mmol), potassium hydroxide (0.5 mmol), anisole as internal reference (0.5 mmol), and catalyst (2.5%) in 0.8 mL of glycerol. The solution was heated to 80−120 °C for the appropriate time. Yields and conversions were determined by GC chromatography during the reaction course. Products and intermediates were characterized by GC/MS. Isolated products were characterized by ^{1}H NMR and ^{13}C NMR after column chromatography purification using *n*-hexane/ethyl acetate mixtures.

General Method for TH under Microwave Irradiation. In a typical experiment, a mixture of substrate (0.5 mmol), catalyst (2.5 mol %), and finely powdered KOH (0.028 g, 0.5 mmol) in glycerol (0.4 mL) was heated under microwave irradiation at 120 °C for 1 h, in a sealed reactor. After cooling, a 2/1 v/v mixture of Et_2O and CH_2Cl_2 (3 mL) was added to the crude product and this mixture was stirred at room temperature for 5 min. The supernatant was recovered, and the operation was repeated three times. The organic phase was dried on $MgSO_4$, filtered, and evaporated under reduced pressure to afford the reduced product as a pure compound. Product conversion was determined by HPLC; the yield was determined by GC/MS.

General Method for TH under Sonication. In a typical experiment, a mixture of substrate (0.5 mmol), catalyst (2.5 mol %), and finely powdered KOH (0.028 g, 0.5 mmol) in glycerol (0.4 mL) was placed in a Pyrex glass reactor and clamped to a vertical support on a magnetic stirrer. The vessel was hold in place such that the tip of the horn was immersed into the reaction mixture to a depth of 1.0 cm and the glass part did not touch the sonochemical probe. The reaction mixture was sonicated at 98 °C continuously for the indicated time (Table 3), with 40% amplitude, while vigorous magnetic stirring was maintained. At the end of the reaction, a 2/1 v/v mixture of Et_2O and CH_2Cl_2 (3 mL) was added to the crude product and this mixture was stirred at room temperature for 5 min. The supernatant was recovered, and the operation was repeated three times. The organic phase was dried on Mg_2SO_4, filtered, and evaporated under reduced pressure to afford the reduced product as a pure compound. Product conversion was determined by HPLC; the yield was determined by GC/MS.

Synthesis of Imidazolium Salt B. A mixture of 1-*n*-butylimidazole (248 mg, 2 mmol) and 3,4,5-trimethoxybenzyl chloride (476 mg, 2.2 mmol) was stirred in a Pyrex tube for 48 h at 95 °C. The brown oil obtained was washed twice with 5 mL of ether, affording an analytically pure product (yield 655 mg, 96%). ^{1}H NMR ($CDCl_3$, 500 MHz): δ 10.31 (s, 1H, H_{imid}), 7.49 (d, $^3J_{H-H}$ = 1.4 Hz, 1H, H_{imid}), 7.24 (d, $^3J_{H-H}$ = 1.5 Hz, 1H, H_{imid}), 6.63 (s, 2H, Ar), 5.21 (s, 2H, NCH_2), 3.97 (t, $^3J_{H-H}$ = 7.4 Hz, 2H, nBu), 3.53 (s, 6H, OCH_3), 3.46 (s, 3H, OCH_3), 1.60−1.48 (m, 2H, nBu), 1.10−0.94 (m, 2H, nBu), 0.59 (t, $^3J_{H-H}$ = 7.5 Hz, nBu). ^{13}C{^{1}H} NMR ($CDCl_3$, 125 MHz): δ 138.1 (C_{imid}) 136.5 (Ar), 129.1 (Ar), 122.4 (Ar), 122.1 (C_{imid}), 121.9 (C_{imid}), 106.3 (Ar), 60.4 (OMe), 56.3 (OMe), 52.9 (NCH_2), 49.5 (nBu), 31.7 (nBu), 19.1 (nBu), 13.1 (nBu). Electrospray MS (cone 15 V; m/z, fragment): 305 $[M - Cl]^+$. HRMS ESI-TOF-MS (positive mode): $[M - Cl]^+$ monoisotopic peak 305.1863, calcd 305.1865, ε_r = 0.7 ppm.

Synthesis of 4A. A suspension of **A** (206 mg, 0.446 mmol) and silver oxide (206 mg, 0.892 mmol) in 1,2-dichloroethane was stirred at 60 °C for 4 h under Ar. After the reaction mixture was cooled to room temperature, $[IrCl(COD)]_2$ (150 mg, 0.223 mmol) was added. The resulting mixture was stirred at room temperature for 48 h under Ar. After solvent removal, CH_2Cl_2 was added to the residue. The resulting suspension was filtered through Celite, and the filtrate was

dx.doi.org/10.1021/om300109e | *Organometallics* 2012, 31, 3911−3919

concentrated to dryness. The product was recrystallized from CH_2Cl_2/hexanes and dried under vacuum, affording a dark orange solid (yield 270 mg, 80%). ^{1}H NMR ($CDCl_3$, 500 MHz): δ 6.72 (s, 4H, Ar), 6.70 (s, 2H, H_{imid}), 6.12 (d, $^2J_{H-H}$ = 14.3 Hz, 2H, NCH_2Ar), 5.14 (d, $^2J_{H-H}$ = 14.3 Hz, 2H, NCH_2Ar), 4.67−4.65 (m, 2H, COD), 3.84 (s, 12H, OCH_3), 3.82 (s, 6H, OCH_3), 3.2−2.9 (m, 2H, COD), 2.21, 2.20 (m, 4H, COD), 1.76−1.74 (m, 4H, COD). $^{13}C\{^1H\}$ NMR ($CDCl_3$, 75 MHz): δ 180.5 (Ir−$C_{carbene}$), 153.5 (Ar), 138.0 (Ar), 131.9 (Ar), 120.5 (CH_{imid}), 105.7 (Ar), 85.2 (COD), 60.8 (OMe), 56.5 (OMe), 54.5 (NCH_2Ar), 51.9 (COD), 33.6 (COD), 29.52 (COD). Anal. Calcd for $C_{31}H_{40}N_2O_6IrCl\cdot C_6H_{14}$ (850.51): C, 52.25; H, 6.40; N, 3.29. Found: C, 52.14; H, 6.78; N, 3.35. Electrospray MS (cone 15 V; *m*/*z*, fragment): 729 $[M - Cl]^+$. HRMS ESI-TOF-MS (positive mode): $[M - Cl]^+$ monoisotopic peak 729.2531, calcd 729.2518, ε_r = 1.7 ppm.

Synthesis of 4B. A suspension of **B** (151 mg, 0.446 mmol) and silver oxide (206 mg, 0.892 mmol) in 1,2-dichloroethane was stirred at 60 °C for 4 h under Ar. After the mixture was cooled to room temperature, $[IrCl(COD)]_2$ (150 mg, 0.223 mmol) was added, and the resulting mixture was stirred at room temperature for 48 h under Ar. After solvent removal, the product was extracted with CH_2Cl_2, filtered through Celite, and concentrated to dryness. The residue was recrystallized from CH_2Cl_2/ hexanes, affording a light yellow solid (yield 227 mg, 78%), ^{1}H NMR ($CDCl_3$, 500 MHz): δ 6.92 (d, $^3J_{H-H}$ = 2.0 Hz, 1H, H_{imid}), 6.71 (d, $^3J_{H-H}$ = 2.0 Hz, 1H, H_{imid}), 6.69 (s, 2H, Ar), 6.06 (d, $^2J_{H-H}$ = 14.4 Hz, 1H, NCH_2-Ar), 5.13 (d, $^2J_{H-H}$ = 14.4 Hz, 1H, NCH_2-Ar), 4.59−4.42 (m, 2H, COD), 4.44−4.37 (m, 2H, nBu), 3.85 (s, 6H, OCH_3), 3.83 (s, 3H, OCH_3), 2.96 (br, 2H, COD), 2.21−2.18 (m, 4H, COD), 1.99−1.93 (m, 2H, nBu), 1.82−1.78 (m, 4H, COD), 1.47−1.45 (m, 2H, nBu), 1.02 (t, $^3J_{H-H}$ = 7.4 Hz, 3H, nBu). $^{13}C\{^1H\}$ NMR ($CDCl_3$, 75 MHz): δ 180.0 (Ir−$C_{carbene}$), 153.5 (Ar), 137.7 (Ar), 132.0 (Ar), 120.5 (CH_{imid}), 119.8 (CH_{imid}), 105.6 (Ar), 84.5 (COD), 84.3 (COD), 60.8 (OMe), 56.4 (OMe), 54.4 (NCH_2Ar), 51.9 (COD), 51.4 (COD), 50.2 (nBu), 33.7 (COD), 33.4 (COD), 32.9 (nBu), 29.7 (COD), 29.4 (COD), 20.0 (nBu), 13.8 (nBu). Anal. Calcd for $C_{25}H_{36}N_2O_3IrCl$ (640.24): C, 46.90; H, 5.67; N, 4.38. Found: C, 46.64; H, 5.73; N, 4.04. Electrospray MS (cone 15 V; *m*/*z*, fragment): 605 $[M - Cl]^+$. HRMS ESI-TOF-MS (positive mode): $[M - Cl]^+$ monoisotopic peak 605.2348, calcd 605.2357, ε = 1.0 ppm.

Synthesis of 5A. A suspension of **A** (116 mg, 0.25 mmol) and silver oxide (116 mg, 0.5 mmol) in 1,2-dichloroethane was stirred at 60 °C for 4 h under Ar. After the mixture was cooled to room temperature, $[Cp^*IrCl_2]_2$ (100 mg, 0.125 mmol) was added and the reaction mixture was stirred at room temperature for 48 h under Ar. After solvent removal, the product was extracted with CH_2Cl_2, filtered through Celite, and concentrated to dryness. The complex was obtained as a brown solid by recrystallization from CH_2Cl_2/hexanes (yield 148 mg, 70%). ^{1}H NMR ($CDCl_3$, 300 MHz): δ 6.74 (s, 2H, H_{imid}), 6.65 (s, 4H, Ar), 6.06 (d, $^3J_{H-H}$ = 14.5 Hz, 2H, NCH_2), 5.09 (d, $^3J_{H-H}$ = 14.4 Hz, 2H, NCH_2), 3.83 (s, 12H, OCH_3), 3.82 (s, 6H, OCH_3), 1.65 (s, 15H, Cp*). $^{13}C\{^1H\}$ NMR ($CDCl_3$, 75 MHz): δ 158.1 (Ir−$C_{carbene}$), 153.5 (Ar), 138.0 (Ar), 132.0 (Ar), 121.7 (CH_{imid}), 106.1 (Ar), 89.0 (Cp), 60.8 (OMe), 56.4 (OMe), 54.8 (NCH_2), 9.2 (Cp). Anal. Calcd for $C_{33}H_{43}N_2O_6IrCl_2\cdot H_2O$ (844.85): C, 46.91; H, 5.37; N, 3.32. Found: C, 47.10; H, 5.78; N, 3.35. Electrospray MS (cone 15 V; *m*/*z*, fragment): 791 $[M - Cl]^+$. HRMS ESI-TOF-MS (positive mode): $[M - Cl]^+$ monoisotopic peak 791.2435, calcd 791.2432, ε_r = 0.3 ppm.

Synthesis of 5B. A suspension of **B** (85 mg, 0.25 mmol) and silver oxide (69 mg, 0.30 mmol) in 1,2-dichloroethane was stirred at 60 °C for 4 h under Ar. After the mixture was cooled to room temperature, $[Cp^*IrCl_2]_2$ (100 mg, 0.125 mmol) was added and the resulting mixture was stirred at room temperature for 48 h under Ar. After solvent removal, the product was extracted with CH_2Cl_2, filtered through Celite, and concentrated to dryness. The product was purified by silica gel column chromatography using a 1 1 v/v CH_2Cl_2/acetone mixture (yield 0.096 g, 55%). ^{1}H NMR ($CDCl_3$, 300 MHz): δ 6.99 (d, $^3J_{H-H}$ = 2.1 Hz, 1H, H_{imid}), 6.78 (d, $^3J_{H-H}$ = 2.1 Hz, 1H, H_{imid}), 6.70 (s, 2H, Ar), 6.17 (d, $^2J_{H-H}$ = 14.4 Hz, 1H, NCH_2), 4.87 (d, $^3J_{H-H}$ = 14.2 Hz, 1H, NCH_2), 4.67−4.61 (m, 2H, nBu), 3.85 (s, 6H, OCH_3), 3.84 (s, 3H, OCH_3), 1.98−1.92 (m, 2H, nBu), 1.63 (s, 15H, Cp*), 1.44−1.39 (m, 2H, nBu), 1.0 (t, $^3J_{H-H}$ = 7.3 Hz, 3H, nBu). $^{13}C\{^1H\}$ NMR ($CDCl_3$, 75 MHz): δ 156.5 (Ir−$C_{carbene}$), 153.5 (Ar), 138.7 (Ar), 132.0 (Ar), 121.7 (CH_{imid}), 120.9 (CH_{imid}), 106.3 (Ar), 88.8 (Cp), 60.8 (OMe), 56.4 (OMe), 54.7 (NCH_2Ar), 50.8 (nBu), 33.7 (nBu), 20.2 (nBu), 13.9 (nBu), 9.2 (Cp). Anal. Calcd for $C_{27}H_{39}N_2O_3IrCl_2\cdot C_6H_{14}$ (788.91): C, 50.24; H, 6.77; N, 3.55. Found: C, 49.93; H, 6.78; N, 3.65. Electrospray MS (cone 15 V; *m*/*z*, fragment): 667 $[M - Cl]^+$. HRMS ESI-TOF-MS (positive mode): $[M - Cl]^+$ monoisotopic peak 667.2273, calcd 667.2272, ε_r = 0.2 ppm.

■ ASSOCIATED CONTENT

Ⓢ Supporting Information

Text, figures, tables, and CIF files giving general procedures, details of the catalytic studies, and ESIMS, HRMS, and X-ray diffraction data. This material is available free of charge via the Internet at http://pubs.acs.org.

■ AUTHOR INFORMATION

Corresponding Author

*J.A.M.: e-mail, jmata@qio.uji.es; fax, (+34) 964728214; tel, (+34) 964729166. E.C.: e-mail, evelina.colacino@univ-montp2.fr; fax, +33 (0)467144866; tel, +33 (0)467144285.

Notes

The authors declare no competing financial interest.

■ ACKNOWLEDGMENTS

We thank the financial support from the Ministerio de Ciencia e Innovación of Spain (CTQ2011-24055) and Bancaixa (P1.1B2010-02 and P1.1B2008-16). We also thank the "Generalitat Valenciana" for a fellowship (A.A.). We are grateful to the Serveis Centrals d'Instrumentació Científica (SCIC) of the Universitat Jaume I for providing us with spectroscopic facilities and to M. Franck Godiard of the "Service Commun de Microscopie Electronique et Analytique" of the University of Montpellier II (France) for TEM analysis and fruitful discussions. We also acknowledge the CNRS and MESR (France) for financial support.

■ REFERENCES

(1) (a) Baig, R. B. N.; Varma, R. S. *Chem. Soc. Rev.* **2012**, *41*, 1559. (b) Barge, A.; Tagliapietra, S.; Tei, L.; Cintas, P.; Cravotto, G. *Curr. Org. Chem.* **2008**, *12*, 1588. (c) Deshmukh, R. R.; Rajagopal, R.; Srinivasan, K. V. *Chem. Commun.* **2001**, 1544. (d) Caddick, S. *Tetrahedron* **1995**, *51*, 10403. (e) Larhed, M.; Moberg, C.; Hallberg, A. *Acc. Chem. Res.* **2002**, *35*, 717. (f) Lidstrom, P.; Tierney, J.; Wathey, B.; Westman, J. *Tetrahedron* **2001**, *57*, 9225. (g) Piermattei, A.; Karthikeyan, S.; Sijbesma, R. P. *Nat. Chem.* **2009**, *1*, 133. (h) Cravotto, G.; Cintas, P. *Chem. Soc. Rev.* **2006**, *35*, 180. (i) Kappe, C. O. *Angew. Chem., Int. Ed. Engl.* **2004**, *43*, 6250. (j) Kappe, C. O. *Chem. Soc. Rev.* **2008**, *37*, 1127. (k) Varma, R. S. *Green Chem.* **2008**, *10*, 1129.

(2) Palmisano, G.; Bonrath, W.; Boffa, L.; Garella, D.; Barge, A.; Cravotto, G. *Adv. Synth. Catal.* **2007**, *349*, 2338.

(3) (a) *The Future of Glycerol*; 2nd ed.; Pagliaro, M., Rossi, M., Eds.; RSC Publishing: Cambridge, U.K., 2010. (b) Gu, Y. L.; Jerome, F. *Green Chem.* **2010**, *12*, 1127. (c) Diaz-Alvarez, A. E.; Francos, J.; Lastra-Barreira, B.; Crochet, P.; Cadierno, V. *Chem. Commun.* **2011**, *47*, 6208. (d) Wolfson, A.; Dlugy, C.; Shotland, Y. *Environ. Chem. Lett.* **2007**, *5*, 67.

(4) (a) Armaroli, N.; Balzani, V. *Angew. Chem., Int. Ed.* **2007**, *46*, 52. (b) Chheda, J. N.; Huber, G. W.; Dumesic, J. A. *Angew. Chem., Int. Ed.* **2007**, *46*, 7164. (c) Corma, A.; Iborra, S.; Velty, A. *Chem. Rev.* **2007**, *107*, 2411. (d) Gu, Y.; Azzouzi, A.; Pouilloux, Y.; Jerome, F.; Barrault, J. *Green Chem.* **2008**, *10*, 164. (e) Soares, R. R.; Simonetti, D. A.; Dumesic, J. A. *Angew. Chem., Int. Ed.* **2006**, *45*, 3982. (f) Painter, R.

M.; Pearson, D. M.; Waymouth, R. M. *Angew. Chem., Int. Ed.* **2010**, *49*, 9456. (g) Bakhrou, N.; Lamaty, F.; Martinez, J.; Colacino, E. *Tetrahedron Lett.* **2010**, *51*, 3935.
(5) (a) Farnetti, E.; Kaspar, J.; Crotti, C. *Green Chem.* **2009**, *11*, 704. (b) Wolfson, A.; Dlugy, C.; Shotland, Y.; Tavor, D. *Tetrahedron Lett.* **2009**, *50*, 5951. (c) Diaz-Alvarez, A. E.; Crochet, P.; Cadierno, V. *Catal. Commun.* **2011**, *13*, 91. (d) Tavor, D.; Sheviev, O.; Dlugy, C.; Wolfson, A. *Can. J. Chem.* **2010**, *88*, 305. (e) Azua, A.; Mata, J. A.; Peris, E. *Organometallics* **2011**, *30*, 5532.
(6) (a) Tavor, D.; Popov, S.; Dlugy, C.; Wolfson, A. *Org. Commun.* **2010**, *3*. (b) Cravotto, G.; Orio, L.; Gaudino, E. C.; Martina, K.; Tavor, D.; Wolfson, A. *ChemSusChem* **2011**, *4*, 1130.
(7) Crotti, C.; Kaspar, J.; Farnetti, E. *Green Chem.* **2010**, *12*, 1295.
(8) Corberan, R.; Mas-Marza, E.; Peris, E. *Eur. J. Inorg. Chem.* **2009**, 1700.
(9) (a) Albrecht, M.; Miecznikowski, J. R.; Samuel, A.; Faller, J. W.; Crabtree, R. H. *Organometallics* **2002**, *21*, 3596. (b) Azua, A.; Sanz, S.; Peris, E. *Organometallics* **2010**, *29*, 3661. (c) Azua, A.; Sanz, S.; Peris, E. *Chem. Eur. J.* **2011**, *17*, 3963. (d) Sanz, S.; Azua, A.; Peris, E. *Dalton Trans.* **2010**, *39*, 6339. (e) Sanz, S.; Benitez, M.; Peris, E. *Organometallics* **2010**, *29*, 275.
(10) Arduengo, A. J. (DuPont) U.S. Patent 5 077 414, 1991.
(11) Ohta, H.; Fujiharaa, T.; Tsuji, Y. *Dalton Trans.* **2008**, 379.
(12) (a) Fujita, K.; Yamaguchi, R. *Synlett* **2005**, 560. (b) Corberan, R.; Peris, E. *Organometallics* **2008**, *27*, 1954.
(13) Zsigmond, A.; Notheisz, F.; Csjernyik, G.; Backvall, J. E. *Top. Catal.* **2002**, *19*, 119.
(14) (a) *Microwave Assisted Organic Chemistry*; Terney, J. P., Lindstrom, P., Eds.; Blackwell Publishing: Oxford, U.K., 2005. (b) Wang, H. M. J.; Lin, I. J. B. *Organometallics* **1998**, *17*, 972.
(15) (a) Cravotto, G.; Cintas, P. *Angew. Chem., Int. Ed.* **2007**, *46*, 5476. (b) Cravotto, G.; Cintas, P. *Chem. Sci.* **2012**, *3*, 295. (c) *Chemistry with Ultrasounds*; Mason, T. J., Ed.; Elsevier Applied Science: London, U.K., 1990; Vol. *28*. (d) *Sonochemistry: the Uses of Ultrasounds in Chemistry*; Mason, T. J., Ed.; RSC Publishing: Cambridge, U.K., 1990. (e) Cravotto, G.; Cintas, P. *Angew. Chem., Int. Ed.* **2007**, *46*, 5476.
(16) Leadbeater, N. E.; Pillsbury, S. J.; Shanahan, E.; Williams, V. A. *Tetrahedron* **2005**, *61*, 3565.
(17) Perreux, L.; Loupy, A. *Tetrahedron* **2001**, *57*, 9199.
(18) Garner, H. R.; Ohkawa, T.; Tuason, O.; Lee, R. L. *Phys. Rev. A* **1990**, *42*, 7264.
(19) (a) *Applied Sonochemistry: Uses of Power Ultrasound in Chemistry and Processing*; Mason, T. J., Lorimer, J., Eds.; Wiley-VCH: Weinheim, Germany, 2002. (b) *Practical Sonochemistry/Power Ultrasound Uses and Applications*; 2nd ed.; Mason, T. J., Peters, D., Eds.; Woodhead Publishing: Cambridge, U.K., 2002; Vol. *1*.
(20) Grace, A. N.; Pandian, K. *Mater. Chem. Phys.* **2007**, *104*, 191.
(21) Komarneni, S.; Li, D. S.; Newalkar, B.; Katsuki, H.; Bhalla, A. S. *Langmuir* **2002**, *18*, 5959.
(22) Crabtree, R. H. *Chem. Rev.* **2012**, *112*, 1536.
(23) Kundu, S.; Liang, H. *J. Colloid Interface Sci.* **2011**, *354*, 597.
(24) Clark, R. C.; Reid, J. S. *Acta Crystallogr., Sect. A* **1995**, *51*, 887.
(25) (a) Sheldrick, G. M. *Acta Crystallogr., Sect. A* **2008**, *64*, 112. (b) Dolomanov, O. V.; Bourhis, L. J.; Gildea, R. J.; Howard, J. A. K.; Puschmann, H. *J. Appl. Crystallogr.* **2009**, *42*, 339.